

NPS ARCHIVE
1962
MAXIM, R.

CONVECTIVE HEAT TRANSFER AND FLOW FRICTION
CHARACTERISTICS OF COMPACT HEAT
EXCHANGER SURFACES

RODNEY E. MAXIM

[Add to Shopping Cart](#)[Save for Later](#)

Technical Reports Collection

Citation Format: Full Citation (1F)

Accession Number :

AD0482250

Citation Status:

Active

Citation Classification:

Unclassified

Field(s) & Group(s):

130100 - AIR CONDITION, HEATING, LIGHTING & VENTILATING

200400 - FLUID MECHANICS

201300 - THERMODYNAMICS

Corporate Author:

NAVAL POSTGRADUATE SCHOOL MONTEREY CA

Unclassified Title:CONVECTIVE HEAT TRANSFER AND FLOW FRICTION CHARACTERISTICS OF
COMPACT HEAT EXCHANGER SURFACES.**Title Classification:**

Unclassified

Descriptive Note:

Master's thesis,

Personal Author(s):

Maxim, Rodney E.

Report Date:

01 Jan 1962

Media Count:

47 Page(s)

Cost:

\$7.00

Report Classification:

Unclassified

Descriptors:

*HEAT EXCHANGERS, *CONVECTION(HEAT TRANSFER), FLUID DYNAMICS, FRICTION, HEAT TRANSFER COEFFICIENTS, FINS, METAL PLATES, SURFACE TARGETS, VOLUME, THEORY, PRESSURE, POROUS METALS, REYNOLDS NUMBER, AIR, STAINLESS STEEL, ALUMINUM, EXPERIMENTAL DATA, COMPUTER PROGRAMMING, TABLES(DATA)

Identifiers:

FLOW FRICTION, SCREENS, STANTON NUMBER, STEEL 1050, STEEL 430.

Abstract:

The experimental results for convective heat transfer and flow friction characteristics of some screen, plate-fin and skewed fin matrices of various geometry are presented. The heat transfer data were obtained using the transient technique. The results, which are presented in graphic and tabular form, should be of practical use for compact heat exchanger design. The tabular results of a digital computer solution giving the maximum slope of the generalized heating curve as a unique function of NTU are appended.

Abstract Classification:

Unclassified

Annotation:

Convective heat transfer and flow friction characteristics of compact heat exchanger surfaces.

Distribution Limitation(s):

01 - APPROVED FOR PUBLIC RELEASE

Source Code:

251450

Document Location:

DTIC

Change Authority:

ST-A USNPS LTR, 23 SEP 71



CONVECTIVE HEAT TRANSFER
AND FLOW FRICTION CHARACTERISTICS
OF COMPACT HEAT EXCHANGER
SURFACES

Rodney E. Maxim

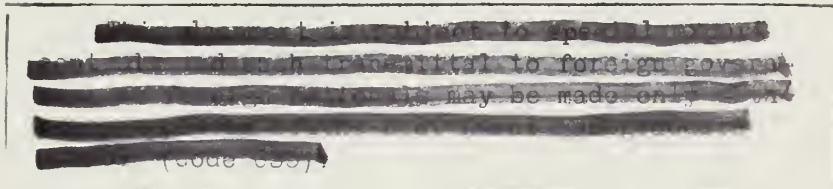
CONVECTIVE HEAT TRANSFER
AND FLOW FRICTION CHARACTERISTICS
OF COMPACT HEAT EXCHANGER

REPORT

by

Rodney E. Maxim

Lieutenant, United States Navy



Submitted in partial fulfillment of
the requirements for the degree of

MASTER OF SCIENCE
IN
MECHANICAL ENGINEERING

United States Naval Postgraduate School
Monterey, California

1 9 6 2

~~MISSISSIPPI~~
MISSISSIPPI
C.D.

NPS ARCHIVE
1962
MAXIM, R

[REDACTED]

CONVECTIVE HEAT TRANSFER
AND FLOW FRICTION AND CHARACTERISTICS
OF COMPACT HEAT EXCHANGER SURFACES

by

Frederic J. Maxin

This work is accepted as fulfilling
the thesis requirements for the degree of

MASTER OF SCIENCE

IN

MECHANICAL ENGINEERING

from the

United States Naval Postgraduate School

ABSTRACT

The experimental results for convective heat transfer and flow friction characteristics of some screen, plate-fin and skewed fin matrices of various geometry are presented. The heat transfer data were obtained using the transient technique.

The results, which are presented in graphic and tabular form, should be of practical use for compact heat exchanger design.

The results of a digital computer solution giving the maximum slope of the generalized heating curve as a unique function of NTU are presented in tabular form in Appendix II.

The author wishes to thank Professor C. P. Howard of the U. S. Naval Postgraduate School for his encouragement and guidance, and Lt. J. A. Inglis, RCN, for solving the Bessel's function and theoretical generalized heating curve equation. The assistance of J. S. Beck and K. Mothersell in fabricating the equipment used is also acknowledged.

TABLE OF CONTENTS

TITLE	PAGE
Abstract	ii
Table of Contents	iii
List of Illustrations	iv
List of Tables	v
List of Symbols and Abbreviations	vi
Introduction	1
Experimental Apparatus	3
Method	6
a. Summary of Theory	6
b. Experimental Technique	8
c. Presentation of Results	9
d. Limitations and Uncertainties	10
Discussion of Results	15
Conclusions	20
Bibliography	21
Appendix I, Sample Calculations, Run #1, Aluminum Plate-Fin	41
Appendix II, Solution of the Generalized Heating Curve Versus T/Z	46

CONTENTS

	PAGE
1. $N_{St} N_{Pr}^{2/3}$ and f' versus N_{Re} for 10 x 10 x .025 18/8 Stainless Steel Screen Matrix	22
2. $N_{St} N_{Pr}^{2/3}$ and f' versus N_{Re} for 60 x 60 x .007 18/8 Stainless Steel Screen Matrix	23
3. $N_{St} N_{Pr}^{2/3}$ and f' versus N_{Re} for 430 Stainless Steel Plate-Fin Matrix	24
4. $N_{St} N_{Pr}^{2/3}$ and f' versus N_{Re} for Aluminum Plate-Fin Matrix	25
5. $N_{St} N_{Pr}^{2/3}$ and f' versus N_{Re} for 25° Skewed Aluminum Fin Matrix	26
6. Best Interpretation of $N_{St} N_{Pr}^{2/3}$ versus N_{Re} Three Matrices	27
7. Best Interpretation of f' versus N_{Re} of These Matrices	28
8. Schematic Diagram of Apparatus	29
9. Photograph of 10 x 10 Screen Matrix	30
10. Photograph of Plate-Fin Matrix	31
11. Photograph of Skewed Fin Matrix	32

LIST OF TABLES

TABLE		PAGE
I	Heat Transfer and Friction Data, 10 x 10 Mesh Per Inch-0.025 Inch Wire Diameter Screen Matrix	33
II	Heat Transfer and Friction Data, 60 x 60 Mesh Per Inch-.007 Inch wire Diameter Screen Matrix	34
III	Heat Transfer Data, Stainless Steel Plate-Fin Matrix	35
IV	Friction Data, Stainless Steel Plate-Fin Matrix	36
V	Heat Transfer and Friction Data, Aluminum Plate-Fin Matrix	37
VI	Heat Transfer and Friction Data, Aluminum Fin-25° Skew Matrix	38
VII	Details of Screen Matrices	39
VIII	Details of Fin Matrices	40
IX	Values of Max. Slope of Generalized Heating Curve, NTU and τ_0 /NTU	47

LIST OF SYMBOLS AND ABBREVIATIONS

English Letter Symbols

- A - matrix heat transfer area, ft^2
- A_c - matrix free flow area, ft^2
- A_s - matrix conduction area, ft^2
- c - specific heat at constant pressure, $\text{BTU}/(\text{lbm}\cdot^\circ\text{F})$
- d - orifice diameter, ft
- D - pipe diameter, ft
- D_h - hydraulic diameter, $(4r_h)$, ft
- ξ_c - dimensional constant, $32.2 \frac{\text{lbm}\cdot\text{ft}}{\text{lb}\cdot\text{sec}^2}$
- G - mass velocity, $\text{lbm}/(\text{hr}\cdot\text{ft}^2)$
- h - unit conductance for thermal convection heat transfer, $\text{BTU}/\text{hr}\cdot\text{ft}^2\cdot^\circ\text{F}$
- k - unit thermal conductivity, $\text{BTU}/\text{hr}\cdot\text{ft}\cdot^\circ\text{F}$
- L - total matrix flow length, ft.
- p - porosity, ratio of void volume to total volume
- P - pressure, lb/ft^2
- r_h - hydraulic radius, $(A_c L/A)$, ft.
- t - temperature, $^\circ\text{F}$.
- v - specific volume, ft^3/lbm
- w - mass flow rate, lbm/hr
- W - mass, lbm
- x - distance from the entrance of a core to a given cross section, measured in direction of flow, ft.
- Z - generalized position variable, $Z = \frac{hA}{w c_p} \cdot \frac{x}{L}$

Greek Letter Symbols

α - heat transfer area per unit volume, ft^2/ft^3

Δ - denotes difference

μ - viscosity, lbm/hr-ft

τ - generalized time variable, $= \frac{hA}{W_s c_s} \left(\theta - \frac{W_s}{W_f} \cdot \frac{x}{L} \right)$

θ - time, hrs.

Dimensionless Groupings

N_{Re} - Reynolds number, $4r_h G/\mu$ (a flow modulus)

N_{St} - Stanton number, $\frac{h}{G c_f}$ (a heat transfer modulus)

N_{Pr} - Prandtl number (a fluid properties modulus)

NTU - number of heat transfer units of a matrix, $\frac{hA}{W_f c_f}$
(a heat transfer parameter)

f - 'Fanning' friction factor, $\frac{\Delta P_{\text{matrix}}}{2g_c} \frac{A}{c} / G^2 v_f^A$

Superscript

' - for perfect stacking

Subscripts

f - fluid phase

i - matrix initial state

s - solid phase

1 - fluid state upstream of matrix

2 - fluid state downstream of matrix

INTRODUCTION

There are two courses open to the designer of a compact heat exchanger for the transfer of a fixed heat load consistent with an allowable pressure drop utilizing a new type of matrix arrangement that is not covered in present heat transfer literature. A matrix will be defined as a porous solid possessing a high ratio of void surface area to bulk volume, and a void geometry which permits the flow of gas or a liquid through it.

The first course, a trial and error technique, consists of analytically predicting the heat transfer and friction characteristics of the matrix, designing and testing a scale version of the heat exchanger, and modifying the design until the required performance is achieved. The time and cost involved in utilizing this method is generally unacceptable to the designer.

The second method consists of generating the required heat transfer and friction data on a small module, and utilizing the results for the full scale design. This method is quite flexible, since many different matrix arrangements can be tested at minimum cost, and an optimum surface chosen.

One of the satisfactory methods of measuring the convective heat transfer characteristics of porous solids utilizes the so-called transient test technique. This consists of introducing a step function in the temperature of the fluid passing through the matrix, which is initially at uniform temperature, and recording the matrix temperature-time history. Using the results of the

analysis developed by G. L. Locke (1)* for the determination of NTU from the generalized heating curve of maximum temperature gradient versus time, it is then possible to compute the Stanton number. The 'Fanning' friction factor is obtained from the pressure drop across the matrix.

The objectives of this thesis were:

- a. to design, fabricate and evaluate the performance of a test section to utilize the transient method for determining heat transfer coefficients of small modules, and
- b. to obtain the heat transfer coefficients and fluid frictional characteristics of screen, triangular fin and plate-fin matrices of various geometry.

*Numbers in parentheses refer to Bibliography on page 21.

EXPERIMENTAL APPARATUS

A schematic diagram of the apparatus is shown in Fig. 8. Basically, the system consists of a plastic section with a sliding drawer for holding the test matrix, a flow measuring system, a pressure measuring system, a compressor to provide flow through the test section, an air heater, a temperature measuring system and piping.

Flow Rate Control

The compressor is run at a constant rate of approximately 300 c.f.m. A sliding-gate valve on a T-section of the inlet piping of the compressor is used for coarse control of air flow through the test section. There is also a fine control valve for making minor adjustments to the air flow rate. A thin plate orifice section for flow measurement, designed according to A.S.M.E. specifications (3), is included in the inlet piping.

Matrix Heating System

A small blower, with a heating element controlled by a 115-volt, 60-cycle AC 'Variac', is positioned to heat the matrix when the drawer is removed from the plastic test section. A transitional section, with flow stabilizing screens, is attached to the blower to accomplish uniform heating of the matrix.

Temperature Measuring System

A five-thermocouple upstream-temperature probe is located in the center of the pipe approximately midway between the orifice and test section. The upstream-downstream air temperature

difference is measured by these thermocouples, connected in series so as to oppose the 5 center thermocouples of a 13-thermocouple tray located immediately after the matrix.

The thirteen-thermocouple tray may be used independently to find the temperature distribution of the downstream air. All thermocouples used are 30-gauge iron-constantan. The temperature difference and distribution is recorded on a Leeds & Northrup 'Speedomax', Model G, emf recorder with a variable range of from 1-20 mv.

Ambient air temperature is read on a mercury thermometer located at the inlet of the entrance piping.

Sliding Drawer Matrix Holder

The sliding drawer matrix holder is constructed of half-inch thick plastic. It is lined with balsa wood, allowing for a 3.08-inch diameter passage for holding the screen matrix. When testing the triangular fin matrices, a 3.125-inch square passage is provided for holding the matrix.

Pressure Measurement System

The pressure drop across the orifice is measured on a 1/4-inch U-tube manometer filled with water. The pressure drop across the matrix is measured on either a 50-inch differential manometer or an inclined 160 mm. manometer filled with water.

Piping

Ambient air is drawn through a 3.08-inch diameter pipe to the test section. When testing the triangular fin matrices,

a transition piece to a 3.125-inch square was inserted before and after the test section. Galvanized ducting is used between the test section outlet and compressor inlet.

METHOD

A. Summary of Theory

The theoretical analysis of the transient heat transfer behavior of a porous medium was first presented by Shumann in 1929. Shumann considered a homogeneous porous medium at a uniform temperature through which a fluid of the same temperature is flowing. At a certain instant, the temperature of the entering fluid is assumed to change to a higher or lower value. The problem is then to find the temperature of the fluid and solid as functions of time and position in the matrix.

The following idealizations and initial and boundary conditions have to be satisfied in order to simplify the problem:

Idealizations

1. The fluid specific heat and viscosity are constant.
2. The thermal conductivity of both fluid and solid is zero in the direction of flow and is infinite within the fluid and solid in the direction normal to the flow.
3. The flow is steady.
4. The porous solid is homogenous.

Initial and Boundary Conditions

1. At time $\theta = 0$, the temperature of the entering fluid changes instantaneously.
2. Initially, the core is at a uniform temperature.
3. No heat passes the core boundaries.

Shumann found the solutions for the fluid and metal temperatures to be:

$$\frac{t_f - t_i}{t_{f1} - t_i} = e^{-(Z + \tau)} \sum_{n=0}^{\infty} \tau^n \frac{d^n}{d(Z\tau)^n} \left[I_0(2\sqrt{Z\tau}) \right] \quad \text{---1}$$

and

$$\frac{t_s - t_i}{t_{s1} - t_i} = e^{-(Z + \tau)} \sum_{n=1}^{\infty} \tau^n \frac{d^n}{d(Z\tau)^n} \left[I_0(2\sqrt{Z\tau}) \right] \quad \text{---2}$$

Shumann's solution requires that a theoretical curve be generated which will match the experimental curve to determine the heat transfer coefficient.

In 1950, Locke (1) developed a method in which only the maximum slope of the theoretical and experimental curves need comparison. This method eliminates the requirement of a large number of theoretical curves and the possibility of error due to the displacement of the experimental heating curve either vertically or horizontally. Locke derived an expression for the slope of the generalized heating curve for the fluid, (equation 1 above), finding that at $x=L$ for which Z becomes equal to the NTU:

$$\frac{d\left(\frac{t_{f2} - t_i}{t_{f1} - t_i}\right)}{d(\tau/NTU)} = \frac{NTU^2}{\sqrt{NTU\tau}} \left[I_1(2\sqrt{NTU\tau}) \right] e^{-(NTU + \tau)} \quad \text{---3}$$

From this, it was found that the maximum slope of the generalized heating curve is a unique function of NTU. Thus, only the maximum slope of the experimental heating curve need be found in order to obtain the NTU and, thereby, the Stanton number. This method has been used by several investigators, and their results have been compiled by Kays & London (2).

Locke, in his solution of Equation 3, resorted to an approximation of the modified Bessel function which in the low range of the argument was subject to large error. A solution to Equation 3 has been carried out by Lt. J. A. Inglis, RCN, using the exact infinite series of the modified Bessel function, on a CDC 1604 digital computer. The results of this solution are given in Appendix II and were the ones used by the author in reducing his experimental data.

B. Experimental Technique

Ambient air is drawn through the inlet pipe and allowed to flow through the test matrix, while the flow rate is adjusted. After constant flow is established, the sliding drawer containing the matrix is pulled out of the test section and into the heated air stream.

When the matrix temperature is steady, as indicated by monitoring the thermocouples, the drawer is rapidly inserted into the ambient air stream and the experiment is started.

The ambient air temperature, orifice pressure drop and matrix pressure drop are recorded, and the transient upstream to downstream temperature difference is recorded on the Leeds

& Northrup 'Speedomax' Recorder. After the temperature difference has returned to zero, the run is terminated.

The following data are recorded:

- a. atmospheric pressure
- b. atmospheric temperature
- c. upstream to downstream temperature difference
- d. pressure drop across the orifice
- e. pressure drop across the matrix
- f. orifice diameter

In this investigation, the temperature difference between the inlet fluid and the downstream fluid temperature was recorded directly so the maximum slope could be determined from the experimental trace with no replotting. For a complete set of sample calculations, see Appendix I.

C. Presentation of Results

To avoid the confusion often encountered when a large number of arbitrarily defined parameters is used, the same definitions will be applied throughout to the various matrix geometries.

The basic data and results for each surface are presented in both tabular (Tables I - VI) and graphic (Figs. 1-5) forms, as:

$$N_{St} Pr^{2/3} = \phi_2(N_{Re})$$
$$f = \phi_2(N_{Re})$$

The Reynolds number is based on a hydraulic diameter, defined as follows:

$$N_{Re} = \frac{4r_h G}{\mu}$$

with

$$4r_h = D_h = 4A_c L/A, \text{ ft.},$$

$$G = W_f/A_c, \text{ lbm hr-ft}^{-2}$$

The Stanton number is defined as:

$$N_{St} = \frac{h}{Gc_f} = NTU A_c/A$$

where

$$NTU = hA/w_{fcf} = \text{number of heat transfer units of the matrix.}$$

The friction factor is defined on the basis of an equivalent shear force in the flow direction per unit of heat transfer area. Entrance and exit losses are included in the friction factor.

$$f = \Delta P_{\text{matrix}} \frac{2g_c A_c}{G^2} v_f A$$

Actually, Prandtl number was not a test variable, as the working fluid was in all cases air at moderate temperatures. Over a moderate range of Prandtl numbers, the effect of Prandtl number to the 2/3 power is used as an approximation.

D. Limitations and Uncertainties

Care must be used to approach the idealizations and initial and boundary conditions of the theoretical analysis, which are restated below:

Idealizations

1. The fluid specific heat and viscosity are constant.
2. The thermal conductivity of both fluid and solid is zero in the direction of flow and is infinite within the fluid and solid in the direction normal to the flow.
3. The flow is steady.
4. The porous solid is homogenous.

Since the fluid used is air, the first idealization can be approached if temperature differences are small. As the maximum temperature difference is approximately 20° F., the arithmetic average will be plus or minus 1.0% in viscosity and negligible in specific heat.

As for the second idealization, it is recognized that thermal conduction along the flow length occurs and increases as the flow rate is lowered. Its effect can be lowered by shortening, or dividing the length of matrix in the flow direction. Mondt (7) indicates that as the Reynolds number is decreased the conduction effect will be small below an NTU of 11.79, have no effect at $NTU = 11.79$, and increase appreciably as the Reynolds number is further reduced.

In the direction normal to the flow, the conduction is negligible since the temperature gradient at any section is essentially zero. This gives a condition which is equivalent to infinite conductivity.

The third idealization is approached by running the com-

pressor at rated capacity for all runs, so that pulsing does not occur.

The fourth idealization is approached by careful selection of the porous solid to be tested.

Initial and Boundary Conditions

1. At time $\theta = 0$, the temperature of the fluid flowing through the matrix changes instantaneously.
2. Initially, the core is at a uniform temperature.
3. No heat passes the core boundaries.

The first condition can be approached by rapidly introducing the heated matrix into the flow stream of constant-temperature ambient air.

The second condition is satisfied by placing screens in the heater duct to produce a uniform velocity profile of the heated air. The downstream side of the matrix is monitored by a thirteen-thermocouple tray to check for a uniform temperature distribution over the section.

The third condition can only be minimized by careful design of the matrix holder. To lower the transfer of heat from the matrix holder to the matrix on cooling, the matrix holder is lined with balsa wood.

The uncertainties of physical constants in the matrix and duct measurements are listed below:

Quantity	Uncertainty at 20:1 odds
c_s	$\pm 4.0\%$
N_{Pr}	$\pm 1.2\%$
c_f	$\pm 0.4\%$
μ	$\pm 1.0\%$
W_s	negligible
L	$\pm 0.5\%$
A_c	$\pm 1.0\%$
A	$\pm 1.0\%$

Instrumentation uncertainties follow:

Quantity	Uncertainty at 20:1 odds
$t_i - t_{f1}$	$\pm 0.5\%$
$\Delta P_{\text{orifice}}$	$\pm 1.0\%$
ΔP_{matrix}	$\pm 2.0\%$

Following is a summary of the uncertainty analysis of the Reynolds number, friction factor, NTU and Stanton number:

For Repeatability

Quantity	Uncertainty at 20:1 odds
N_{Re}	$\pm 2.0\%$
f	$\pm 3.5\%$
NTU	$\pm 8.0-10\%$
N_{St}	$\pm 8.0-10\%$
$N_{St} N_{Pr}^{2/3}$	$\pm 8.0-10\%$

The NTU, N_{St} and $N_{St}N_{Pr}^{2/3}$ are represented with a variable range of uncertainties because NTU does not vary linearly with the maximum slope of the cooling curve.

NTU	Uncertainty at 20:1 odds
6	$\pm 10\%$
10	$\pm 9.0\%$
16	$\pm 8.0\%$
20	$\pm 9.0\%$

For Reproducibility

Quantity	Uncertainty at 20:1 odds
N_{Re}	$\pm 3.0\%$
f	$\pm 4.0\%$
NTU	$\pm 18-22\%$
N_{St}	$\pm 18-22\%$
$N_{St}N_{Pr}^{2/3}$	$\pm 18-22\%$

NTU	Uncertainty at 20:1 odds
6	$\pm 22\%$
10	$\pm 20\%$
16	$\pm 18\%$
20	$\pm 19\%$

DISCUSSION OF RESULTS

To evaluate the performance of the test section, 60 x 60 x 0.0070 and 10 x 10 x 0.025 18/8 stainless steel screen matrices which were similar to those used by other investigators were tested (see Table VII and Fig. 9). Fig. 1 compares the results of the present investigation with the best interpretation of the data obtained by Coppage and Tong (9) also on 10 x 10 x 0.025 screen matrices. Fig. 2 compares the results of the present investigation of 60 x 60 x 0.0070 screens with the best interpretation of the data obtained by Coppage and Tong on 60 x 60 x 0.0075 screens. The heat transfer and fluid friction characteristics obtained for the screen matrices are well within the range of uncertainty of reproducibility of Coppage, Ton, and the author.

In addition to the screen matrices, which were tested primarily to evaluate the performance of the test section, three different geometry matrices were investigated: two of the plate-fin type (Fig. 10) and one fin type (Fig. 11) in which the elements were skewed to prevent meshing of the fins. Table VIII lists the details of these matrices.

Results for the Type 430 stainless steel plate-fin matrix are shown in Fig. 3 and listed in Tables III and IV. From the figure it is seen that in the higher Reynolds number range, the heat transfer behavior follows the characteristic straight line with a slope of slightly less than the minus one

expected for laminar flow in smooth channels. At a Reynolds number of about 100 and a test NTU of about 15, the data begins to depart from the straight line behavior. As the Reynolds number decreases, this departure becomes more pronounced and finally reaches a point where it appears that the heat transfer coefficient becomes constant or independent of the Reynolds number. This behavior is due to the longitudinal heat conduction within the matrix, and, as mentioned earlier, was expected to start showing up when the NTU theoretically had a value of 11.79(7).

Since the conduction parameter* for a given geometry and material varies inversely as the Reynolds number, the smaller the Reynolds number the greater the effect. The conduction parameter also varies inversely as the flow length, so that a first observation would indicate that decreasing the length does not improve the situation; but, since the NTU is directly proportional to the heat transfer area, decreasing the matrix length sufficiently will decrease the NTU to allow testing a lower Reynolds number range. In this investigation the matrix length was not decreased because it was only desired to establish the straight line laminar flow behavior and sufficient data was obtained to do this without altering the matrix length. Having established the heat transfer behavior in the higher laminar Reynolds number range thus allows extrapolation of the data into the lower Reynolds number range. It should be noted, however, that when

*The conduction parameter is defined as $\frac{kA_s}{w_1 c_p L}$

such information as this is utilized in heat exchanger design, conduction plays an important part in the heat exchanger's performance, and there has been no attempt in this investigation to obtain correlations which would predict the effects of conduction.

The friction factor curve for the Type 430 stainless steel plate fin matrix shows essentially a straight line behavior with a slope approximately that of the heat transfer curve as would be expected for laminar flow conditions.

Results for the aluminum plate-fin matrix are shown in Fig. 4 and Table V. For this matrix the only geometry change was that of the hydraulic diameter, which was accomplished by reducing the fin height and pitch. This change, along with the use of thinner material, provided for a greatly increased ratio of heat transfer area to unit volume and of free flow area to frontal area compared with the Type 430 stainless steel plate-fin matrix. The experimental results show the same type behavior as previously discussed with the conduction effect beginning at a Reynolds number of about 200 where the test NTU was about 13.

In Fig. 5 and Table VI are shown the results for the more radical of the geometry changes. For this matrix the plates were removed leaving only the fins; and to prevent meshing of the fins, the elements were made so that the total angle between two elements' flow channels was 25° . This angle was chosen simply because it was an easy one to fabricate and sufficiently

removed from a zero angle to produce a large effect. It was believed that with such an obviously tortuous flow channel the shape of the result curves would more nearly approach those of the screen matrices. That this was not the case is readily evident by comparing Fig. 5 with either Fig. 1 or 2. Instead, the behavior of this matrix was quite similar to that of the plate-fin type and will be discussed in more detail later. The conduction effect is seen to begin at a Reynolds number of about 300 for which the test NTU was about 12.

For comparison purposes the best interpretation of the heat transfer characteristics of the three finned matrices have been replotted and extended in Fig. 6, and the fluid friction characteristics reproduced in Fig. 7.

Comparing the stainless steel plate-fin and aluminum plate-fin matrices shows the effect of reducing the hydraulic diameter by reducing size and pitch. The smaller finned aluminum matrix has approximately the same fluid friction characteristics as the stainless steel matrix, while the heat transfer characteristics are raised 47%. This would indicate that the fins in plate-fin heat exchangers could be reduced in size to the limit allowed by considerations other than heat transfer.

The comparison of the aluminum plate-fin and skewed fin matrices of the same fin size shows the effect of removing the plate and skewing by 25°. These changes increase the fluid

friction characteristics by 100% and the heat transfer characteristics by 73.5%. Although the heat transfer rate is increased, this may be an expensive means, especially in gas turbine regenerators where a 1% increase in pressure drop due to flow friction costs more than a 1% increase in specific fuel consumption. Possibly there is a skew angle at which the increase in heat transfer characteristics is sufficiently greater than the increase in friction characteristics to warrant its use.

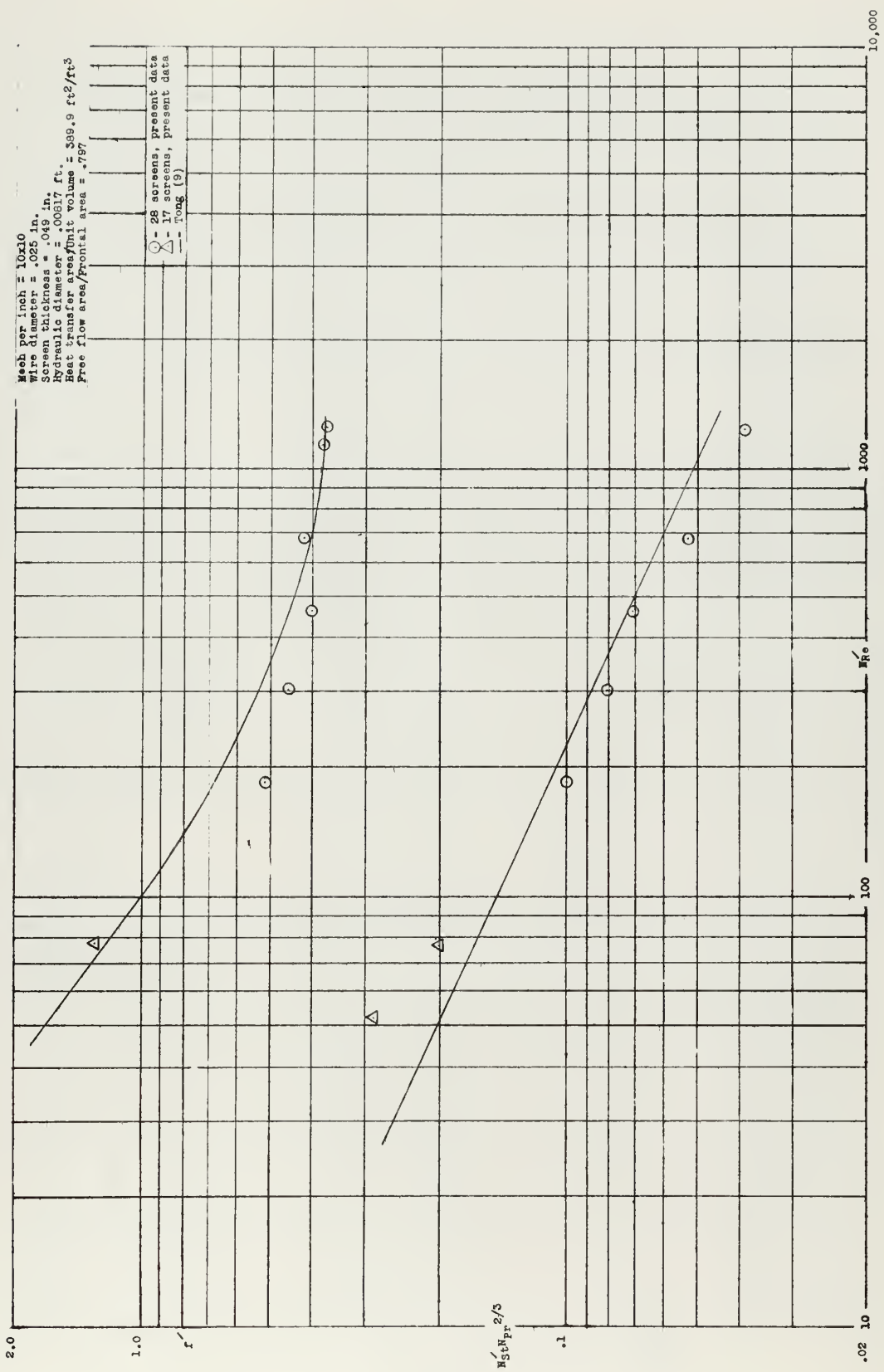
Comparing the stainless steel plate-fin and skewed aluminum fin matrices shows an increase of 159% in the heat transfer characteristics and an increase of as much as 120% in the fluid friction characteristics. In this case, the heat transfer area per unit volume is nearly the same for these surfaces, but the hydraulic diameter for the skewed fins is practically 50% greater, indicating that there would be less chance of fouling with the skewed arrangement.

CONCLUSIONS

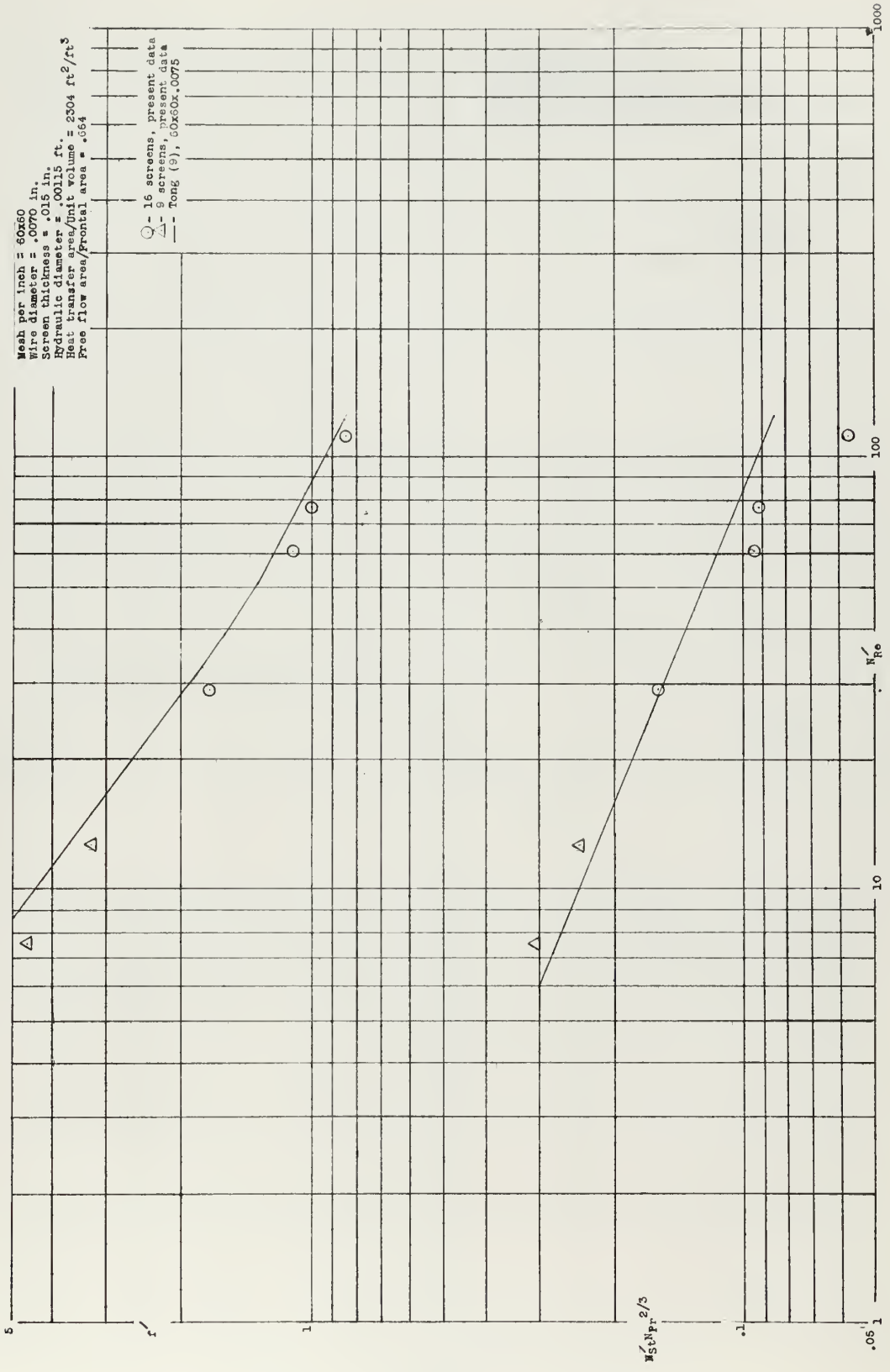
1. A successful test section has been designed and fabricated to obtain convective heat transfer and friction coefficients for small modules.
2. Convective heat transfer and friction coefficients have been obtained for some screen, triangular fin and plate-fin matrices of various geometries.
3. The experimental results of heat transfer behavior and friction factors for the plate-fin and fin matrices, summarized in Figs. 6 and 7, indicate that there may be better geometries for compact heat exchanger applications than plate-fin types for comparable ratios of heat transfer area to unit volume.

BIBLIOGRAPHY

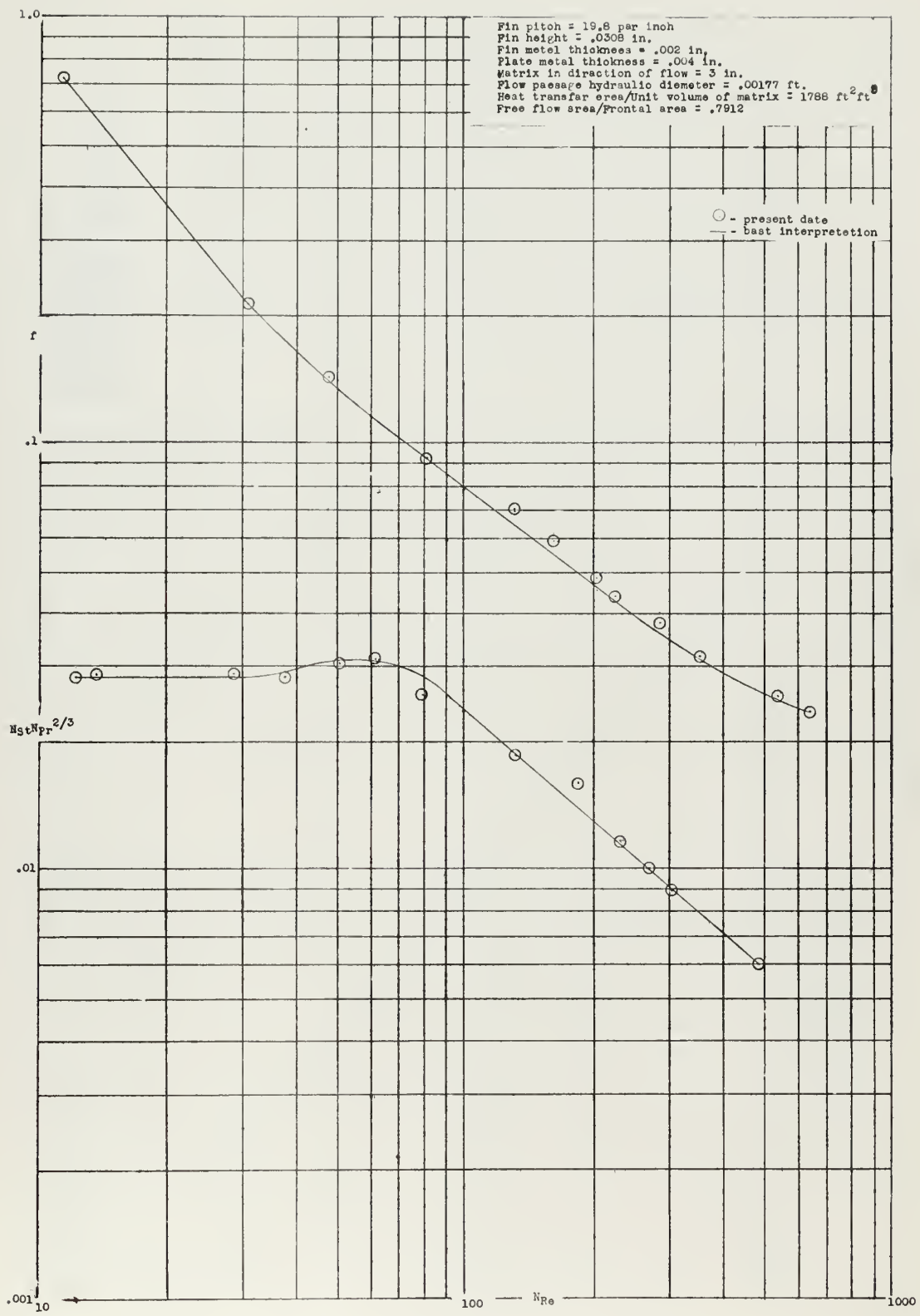
1. Locke, G. L., Heat Transfer and Flow Friction Characteristics of Porous Solids, Technical Report No. 10, Dept. of Mech. Eng., Stanford University (June 1, 1950).
2. W. M. Kays and A. L. London, Compact Heat Exchangers, National Press (1955).
3. Flow Measurement (Ch. 4), Measurement of Quantity of Materials (Part 5), Supplement on Instruments and Apparatus, ASME (1959).
4. St. Ville, Edward L., Lt., USN, Heat Transfer Characteristics of Screen Matrices at Low Reynolds Numbers, USNPS Thesis (1959).
5. A. L. London & W. M. Kays, The Gas Turbine Regenerator--The Use of Compact Heat Transfer Surfaces, pp. 611-621, Vol. 72, ASME (1950).
6. D. C. Briggs and A. L. London, The Heat Transfer and Flow Friction Characteristics of Five Offset Rectangular and Six Plain Triangular Plate-Fin Heat Transfer Surfaces, Technical Report No. 49, Dept. of Mech. Eng., Stanford University (November 30, 1960).
7. Mondt, J. R., Effects of Longitudinal Thermal Conduction in the Solid on Apparent Convection Behavior, with Data for Plate-Fin Surfaces, General Motors Research Laboratory, Warren, Mich.
8. Coppage, J. E., Heat Transfer and Flow Friction Characteristics of Porous Media, Technical Report No. 16, Dept. of Mech. Eng., Stanford University (December 1, 1952).
9. Tong, S. L., Heat Transfer and Friction Characteristics of Screen Matrices at High Reynolds Numbers, Technical Report No. 28, Dept. of Mech. Eng., Stanford University (April 1956).
10. Hilsenrath, J., et al., Tables of Thermal Properties of Gases, U. S. Dept. of Commerce, National Bureau of Standards, Circular 564, Nov. 1955.



$N_{St, Pr}^{2/3}$ and r versus Re for 10x10 x .025 18/8 stainless steel
 Figure 1

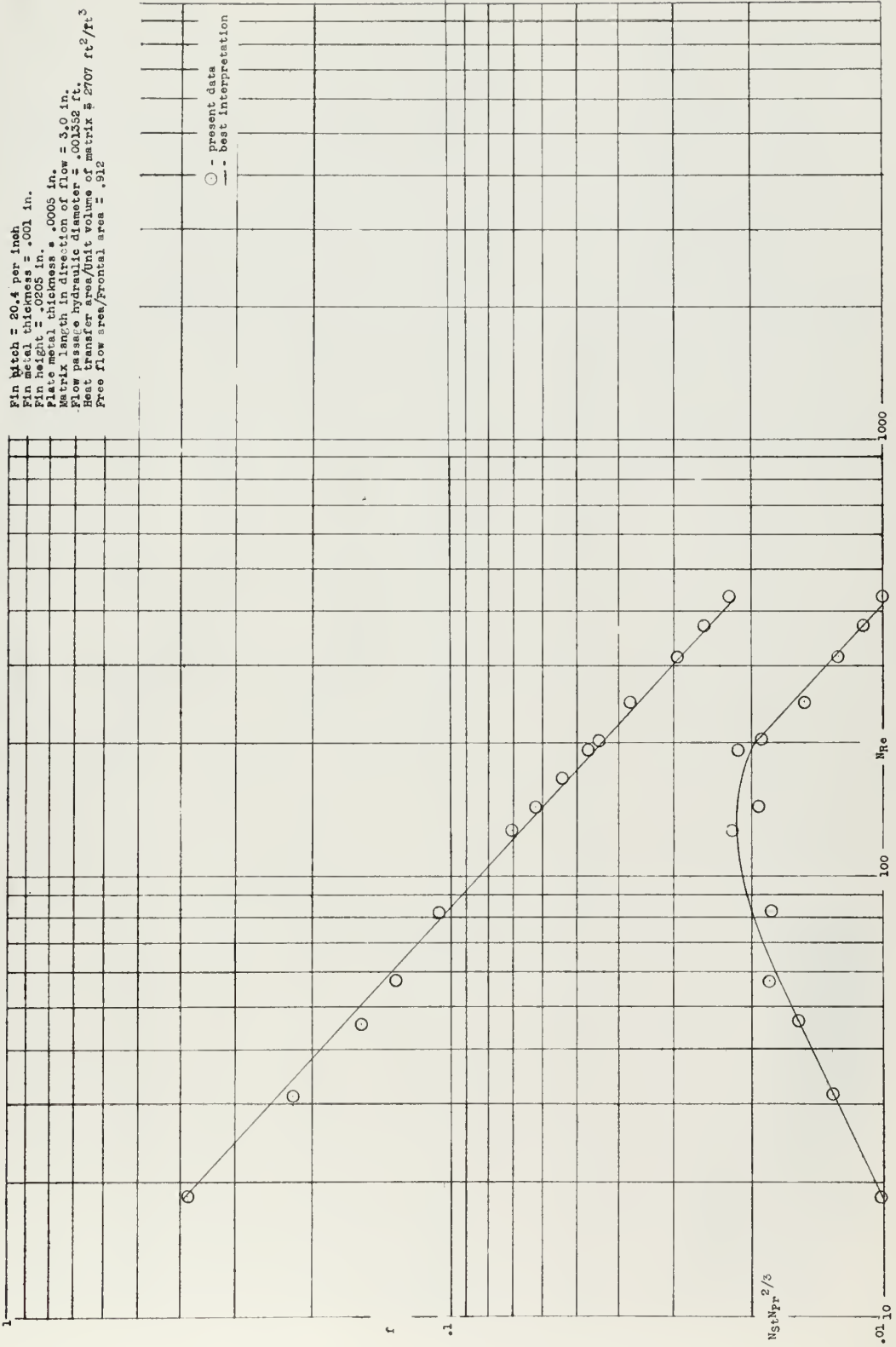


$N_{St} N_{Fr}^{2/3}$ and f' versus N_{Re} for 60x60 x .007 lb/8 stainless steel Figure 2

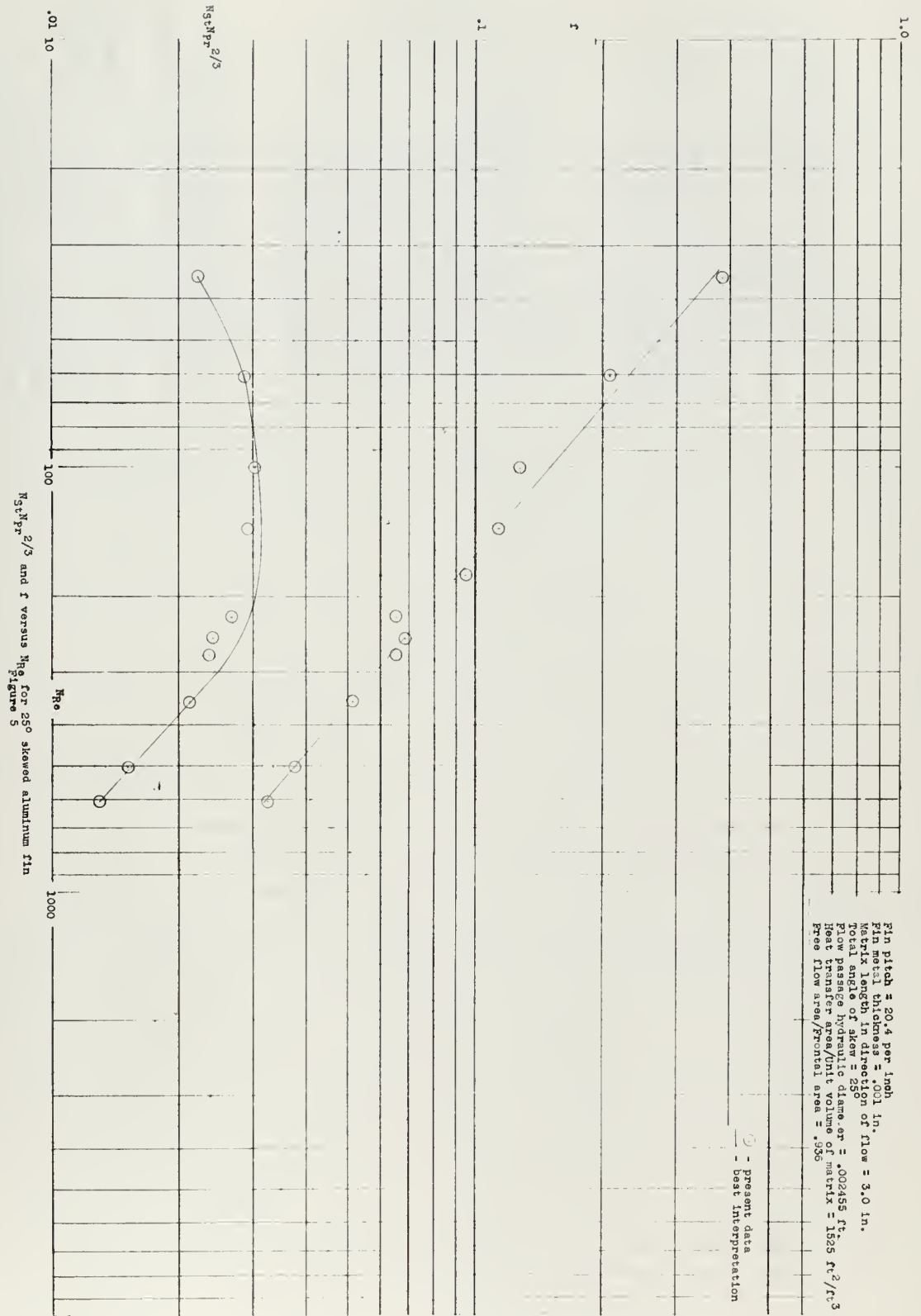


$N_{st}N_{pr}^{2/3}$ and f versus N_{Re} for 430 stainless steel plate-fin
 Figure 3

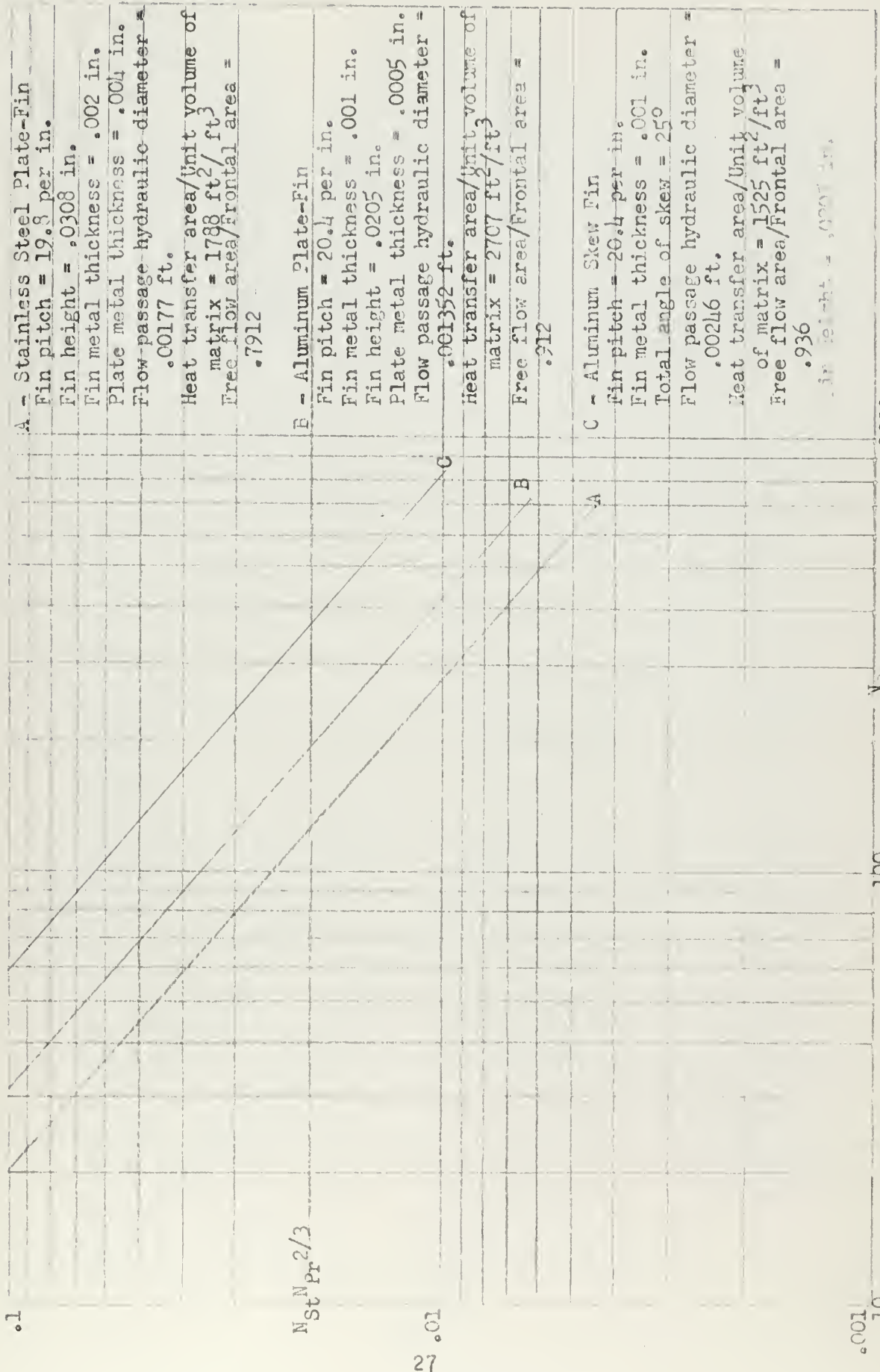
Fin pitch = 20.4 per inch
 Fin metal thickness = .001 in.
 Plate height = .001 in.
 Plate metal thickness = .0005 in.
 Matrix length in direction of flow = 3.0 in.
 Flow passage hydraulic diameter = .00152 ft.
 Heat transfer area/Unit volume of matrix = 2707 ft²/ft.³
 Free flow area/Frontal area = .912



Nu^2/s and f versus Re for aluminum plate-fin
 Figure 4



Nu and f versus Re for 25° skewed aluminum fin
 Figure 5



A - Stainless Steel Plate-Fin
 Fin pitch = 19.8 per in.

Fin height = .0308 in.

Fin metal thickness = .002 in.

Plate metal thickness = .004 in.

Flow passage hydraulic diameter = .00177 ft.

Heat transfer area/Unit volume of matrix = 1788 ft²/ft³

Free flow area/Frontal area = .7912

B - Aluminum Plate-Fin

Fin pitch = 20.4 per in.

Fin metal thickness = .001 in.

Fin height = .0205 in.

Plate metal thickness = .0005 in.

Flow passage hydraulic diameter = .001352 ft.

Heat transfer area/Unit volume of matrix = 2707 ft²/ft³

Free flow area/Frontal area = .912

C - Aluminum Skew Fin

Fin pitch = 26.4 per in.

Fin metal thickness = .001 in.

Total angle of skew = 25°

Flow passage hydraulic diameter = .00246 ft.

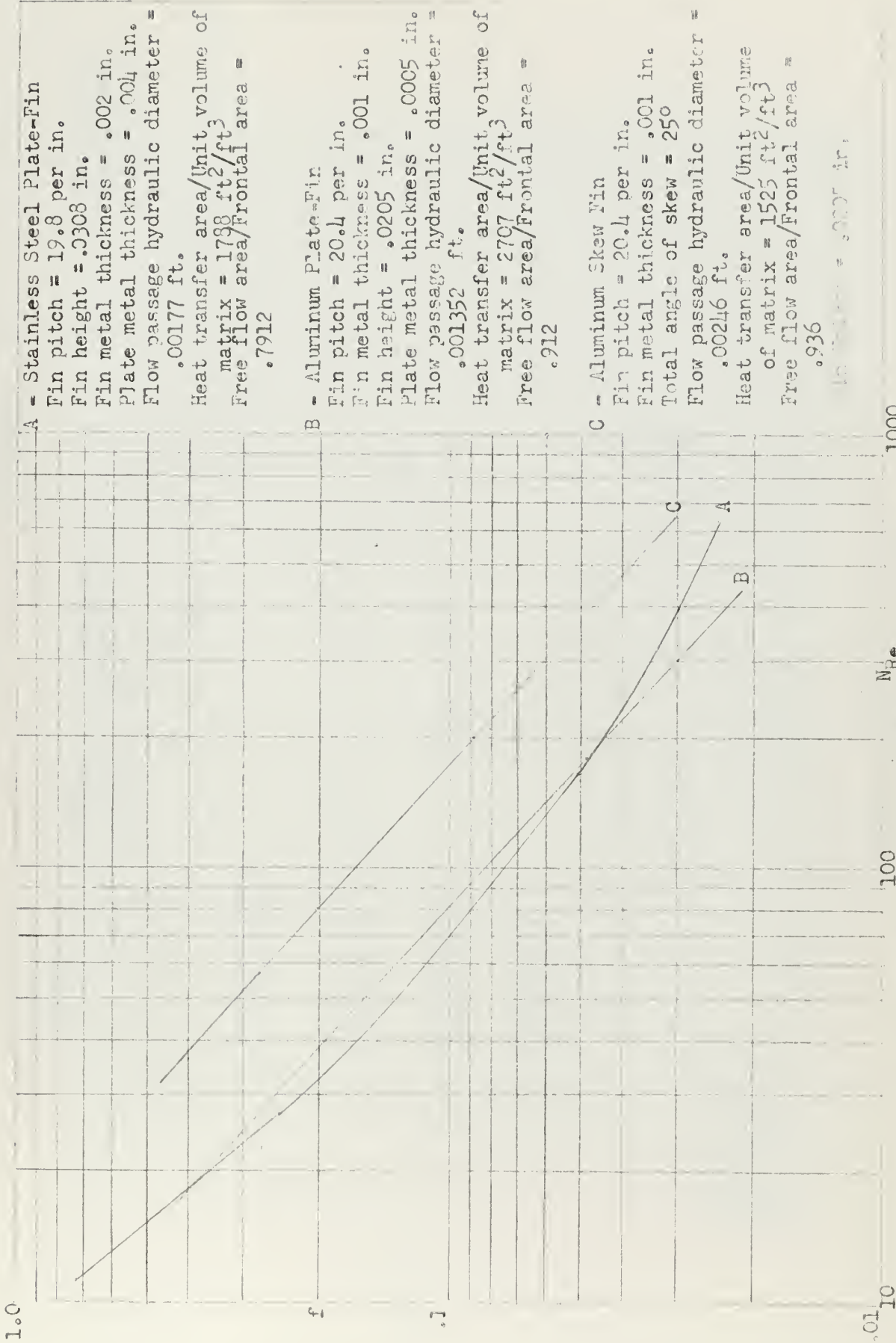
Heat transfer area/Unit volume of matrix = 1525 ft²/ft³

Free flow area/Frontal area = .936

in. height = .0001 ft.

Best Interpretation of $N_{St}N_{Pr}^{2/3}$ versus N_{Re} of Three Matrices

Figure 6



A - Stainless Steel Plate-Fin
 Fin pitch = 19.8 per in.
 Fin height = .0308 in.
 Fin metal thickness = .002 in.
 Plate metal thickness = .004 in.
 Flow passage hydraulic diameter = .00177 ft.
 Heat transfer area/Unit volume of matrix = $1788 \text{ ft}^2/\text{ft}^3$
 Free flow area/Frontal area = .7912

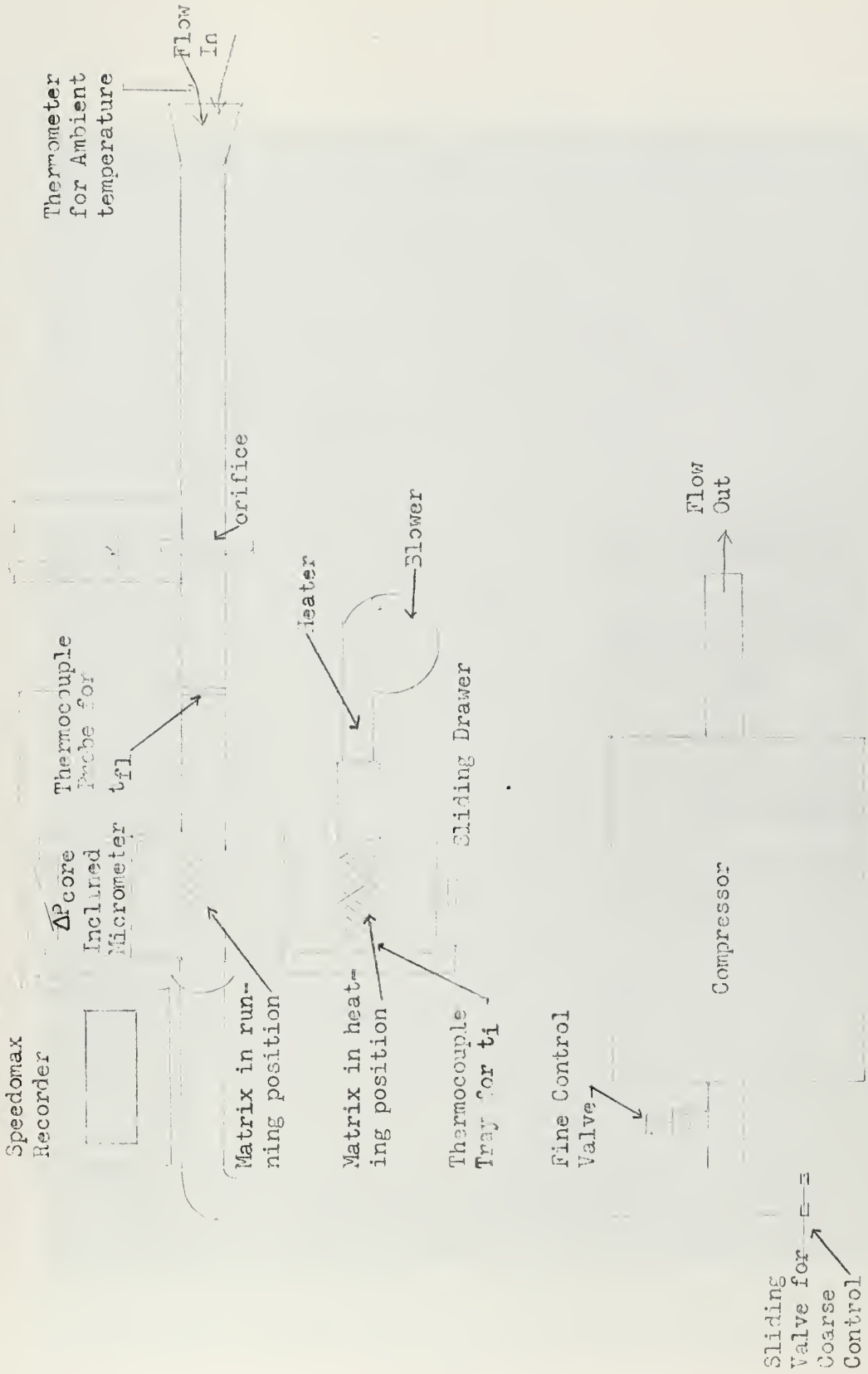
B - Aluminum Plate-Fin
 Fin pitch = 20.4 per in.
 Fin metal thickness = .001 in.
 Fin height = .0205 in.
 Plate metal thickness = .0005 in.
 Flow passage hydraulic diameter = .001352 ft.
 Heat transfer area/Unit volume of matrix = $2707 \text{ ft}^2/\text{ft}^3$
 Free flow area/Frontal area = .912

C - Aluminum Skew Fin
 Fin pitch = 20.4 per in.
 Fin metal thickness = .001 in.
 Total angle of skew = 25°
 Flow passage hydraulic diameter = .00246 ft.
 Heat transfer area/Unit volume of matrix = $1525 \text{ ft}^2/\text{ft}^3$
 Free flow area/Frontal area = .936

Best Interpretation of f versus N_{Re} of Three Matrices
 Figure 7

U tube Manometer

ΔP orifice



Schematic Diagram of Apparatus
Figure 8

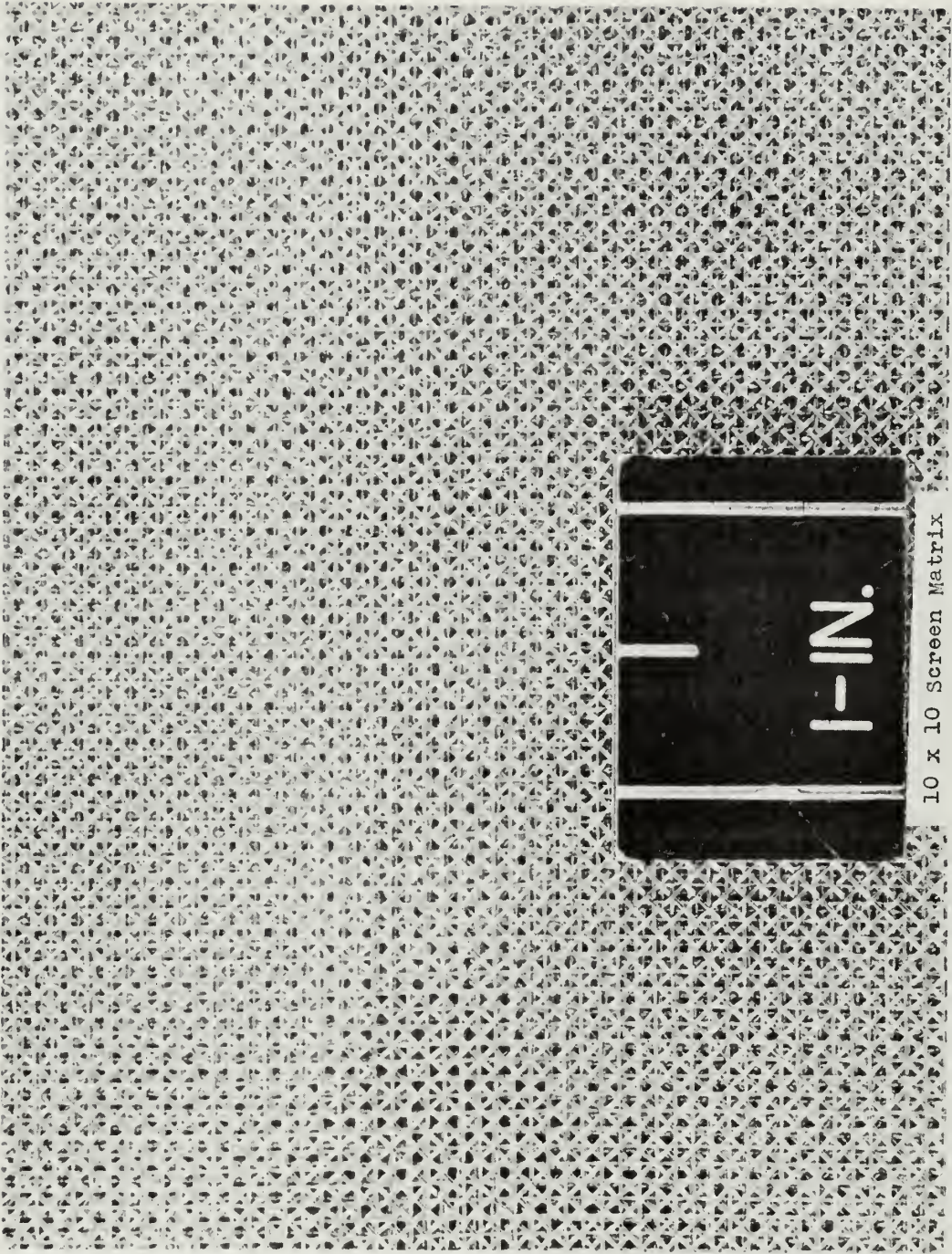


Figure 9

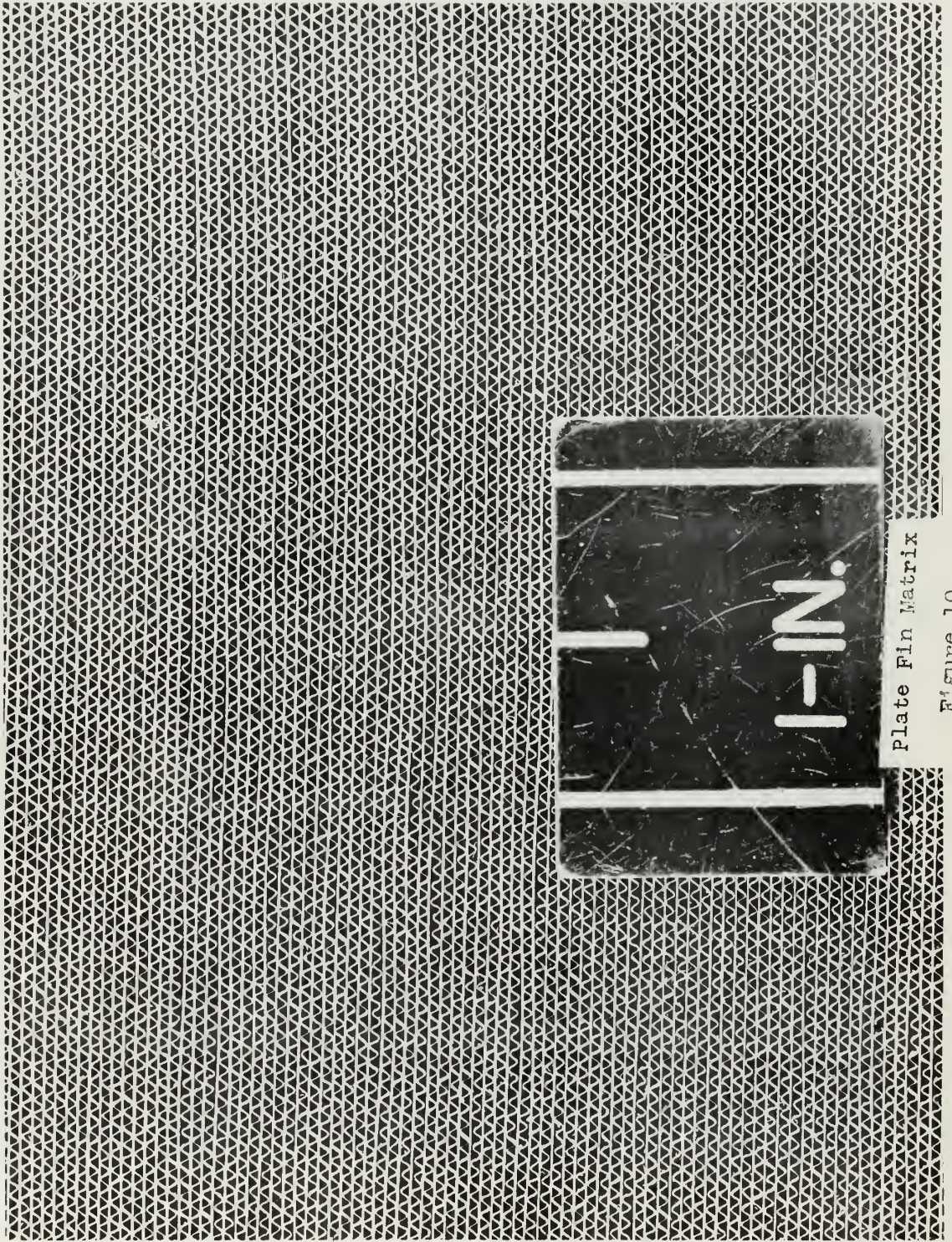
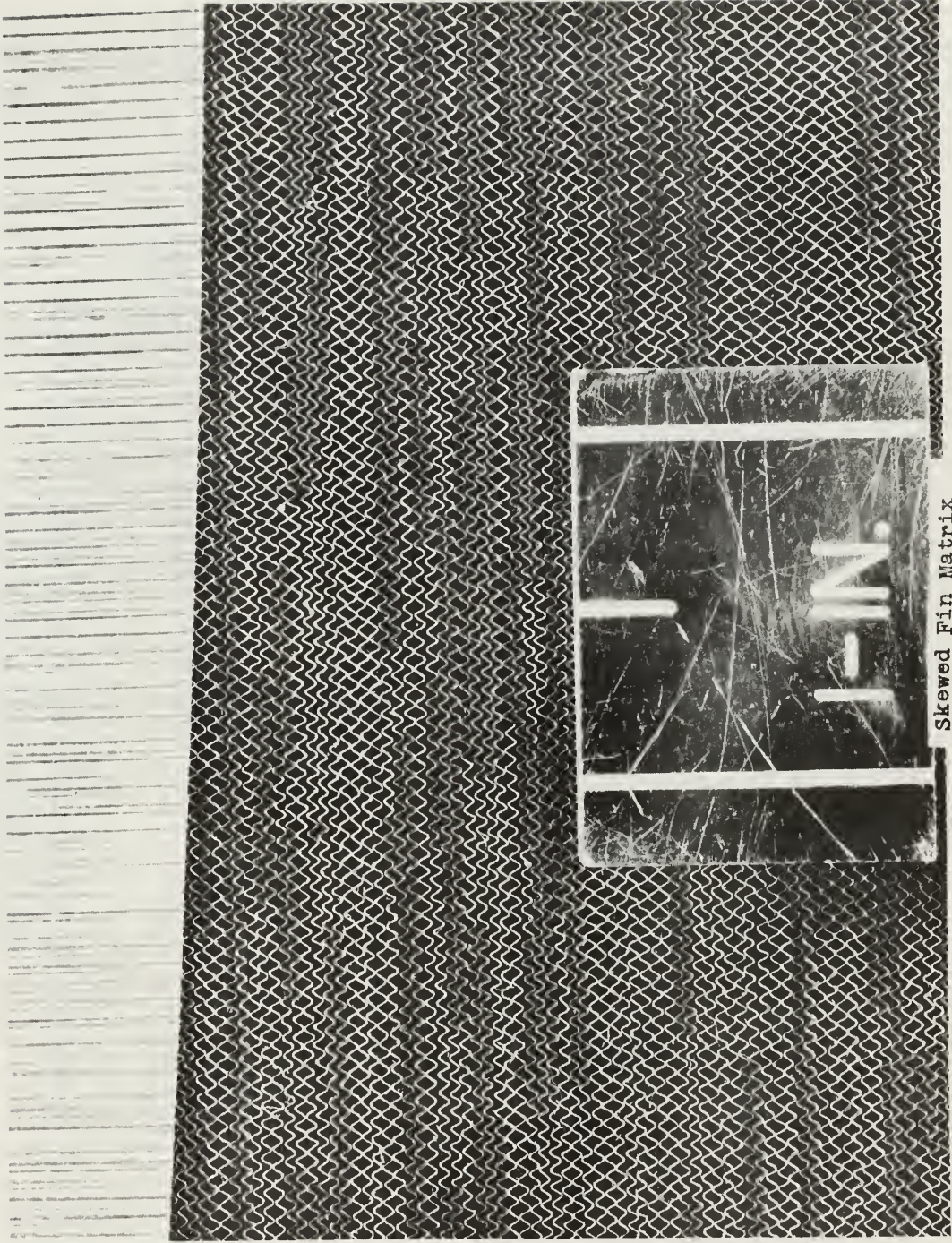


Plate Fin Matrix

Figure 10



Skewed Fin Matrix

Figure 11

TABLE I

HEAT TRANSFER AND FRICTION DATA

10 x 10 MESH PER INCH--0.025 INCH WIRE DIAMETER SCREEN MATRIX

No. of Screens	run	w_f lbm/hr	NTU	N_{Re}	$N_{St} N_{Pr}^{2/3}$	ΔP_{matrix} in. H ₂ O	f'
28	1	275.0	2.75	1240	0.0390	2.88	0.370
	2	256.0		1150		2.54	0.376
	3	151.0	3.71	679	0.0527	0.990	0.420
	4	102.0	5.00	460	0.0710	0.433	0.400
	5	67.2	5.70	302	0.0810	0.212	0.457
	6	41.2	7.00	185	0.0995	0.091	0.520
17	7	17.1	8.60	76.6	0.201		
	8	17.2		77.2		0.041	1.30
	9	11.6	12.3	51.9	0.237		

TABLE II

HEAT TRANSFER AND FRICTION DATA

60 x 60 MESH PER INCH--.0070 INCH WIRE DIAMETER SCREEN MATRIX

<u>No. of Screens</u>	<u>Run</u>	<u>wf lbm/hr</u>	<u>NTU</u>	<u>N_{Re}</u>	<u>N_{St}N_{Pr}^{2/3}</u>	<u>ΔP_{matrix} in. H₂O</u>	<u>f'</u>
16	1	148.0	5.00	113.	0.057	3.45	0.85
	2	101.0	8.02	76.7	0.092	1.89	1.00
	3	80.0	8.20	60.7	0.094	1.31	1.11
	4	38.1	12.6	28.9	0.158	0.46	1.72
9	5	16.7	11.9	12.6	0.242	0.095	3.23
	6	9.9	15.1	7.5	0.307	0.047	4.60

TABLE III

HEAT TRANSFER DATA

STAINLESS STEEL PLATE-FIN MATRIX

\dot{m}_f lbm/hr	NTU	N_{Re}	$N_{St} N_{Pr}^{2/3}$
1	4.32	480	0.0060
2	6.38	301	0.0089
3	7.20	270	0.0100
4	8.37	231	0.0117
5	11.3	184	0.0158
6	13.4	132	0.0187
7	15.5	79.7	0.0259
8	22.0	61.5	0.0307
9	21.7	50.5	0.0304
10	20.2	37.6	0.0283
11	20.8	28.8	0.0290
12	20.7	13.6	0.0290
13	20.2	12.2	0.0283

TABLE IV

FRICTION DATA

STAINLESS STEEL PLATE-FIN MATRIX

<u>run</u>	<u>wf</u> <u>lbm/hr</u>	<u>NRe</u>	<u>ΔP_{matrix}</u> <u>in. H₂O</u>	<u>f</u>
1	809	641	10.5	0.0237
2	632	540	8.05	0.0257
3	451	357	6.10	0.0319
4	359	285	3.33	0.0381
5	283	224	2.39	0.0442
6	253	204	2.20	0.0489
7	203	161	1.66	0.0595
8	165	131	1.30	0.0705
9	103	81.7	0.670	0.0930
10	60.5	47.9	0.350	0.143
11	39.4	31.2	0.220	0.214
12	14.7	11.6	0.106	0.728

TABLE V
HEAT TRANSFER AND FRICTION DATA

ALUMINUM PLATE-FIN MATRIX

<u>Run</u>	<u>wf</u> <u>lbm/hr</u>	<u>NTU</u>	<u>NRe</u>	<u>NStNPr²/3</u>	<u>ΔP_{matrix}</u> <u>in. H₂O</u>	<u>f</u>
1	839	9.17	432	0.0100	10.2	0.0225
2	720	10.1	371	0.0111	8.59	0.0257
3	608	11.7	313	0.0127	7.09	0.0297
4	482	14.0	248	0.0152	5.60	0.0374
5	398	17.4	205	0.0190	4.60	0.0449
6	371	19.7	191	0.0215	4.24	0.0478
7	325		167		3.70	0.0543
8	280	17.7	144	0.0193	3.14	0.0624
9	247	20.3	127	0.0221	2.80	0.0709
10	160	16.6	82.5	0.0131	1.77	0.107
11	111	16.7	57.3	0.0183	1.06	0.133
12	90.4	14.6	46.6	0.0158	0.83	0.157
13	82.7	13.1	42.6	0.0143	0.75	0.170
14	61.9	11.9	31.9	0.0130	0.55	0.223
15	36.0	9.26	18.6	0.0101	0.32	0.384

TABLE VI
HEAT TRANSFER AND FRICTION DATA
ALUMINUM FIN--25° SKEW MATRIX

<u>Run</u>	<u>wf</u> lbm/hr	<u>NTU</u>	<u>Re</u>	<u>$N_{St} N_{Pr}^{2/3}$</u>	<u>$\frac{\Delta P_{matrix}}{in. H_2O}$</u>	<u>f</u>
1	556	6.70	609	0.0130	4.90	0.0325
2	543	7.74	504	0.0151	3.89	0.0376
3	381	11.0	353	0.0214	2.60	0.0513
4	296	12.2	275	0.0237	2.00	0.0651
5	272	12.4	252	0.0241	1.77	0.0686
6	193	11.7	179	0.0229	1.24	0.0950
7	242	13.8	225	0.0269	1.34	0.0654
8	151	15.0	140	0.0292	0.91	0.114
9	108	15.6	100	0.0303	0.52	0.128
10	65.6	14.7	60.9	0.0286	0.32	0.209
11	38.5	11.5	35.8	0.0224	0.15	0.343

TABLE VII

DETAILS OF SCREEN MATRICES

Screen Used	Meshes/inch		Meshes/inch <u>10 x 10</u>
	<u>60 x 60</u>	9	
Number of screens	16	9	28
Wire diameter (in.)	0.0070	0.0070	0.0250
Screen thickness (in.)	0.015	0.015	0.049
Mass (lbm)	0.1703	0.0951	0.588
Porosity, p'	0.664	0.664	0.797
Heat transfer area per unit volume, (ft^2/ft^3)	230	230	390
Hydraulic diameter, D_h (ft.)	0.00115	0.00115	0.00817
Free flow area, A_c (ft^2)	0.0343	0.0343	0.0412
Heat transfer area, A (ft^2)	2.38	1.34	2.31
Length of matrix, L' (in.)	0.240	0.135	1.372

TABLE VIII

DETAILS OF FINNED MATRICES

<u>Designation</u>	<u>Plate-fin</u>	<u>Plate-fin</u>	<u>Skewed fin</u>
Material	Type 430 Stainless steel	Aluminum	Aluminum
Fins per inch	19.8	20.4	20.4
Fin thickness (in.)	0.0020	0.0010	0.0010
Plate thickness (in.)	0.0010	0.0050	0.0010
Fin height (in.)	0.0308	0.0205	0.0205
Length of Matrix (in.)	3.00	3.00	3.00
Mass (lbm)	1.245	0.334	0.185
Heat transfer area per unit volume, (ft^2/ft^3)	1790	2710	1530
Hydraulic diameter, D_h (ft.)	0.00177	0.00135	0.00246
Pre-flow area, A_c (ft^2)	0.0507	0.0594	0.0600
Heat transfer area, A_s (ft^2)	28.60	43.40	24.40
Specific heat, c , ($\frac{\text{BTU}}{\text{lbm}^\circ\text{F}}$)	0.12	0.216	0.210
Porosity, p	0.791	0.912	0.936

APPENDIX I

SAMPLE CALCULATIONS. RUN #1, ALUMINUM FLAT-FIN MATRIX

Recorded Data

$$t_{f1} = 70.0^{\circ}\text{F. (ambient air temperature)}$$

$$\Delta P_{\text{orifice}} = 4.62 \text{ in. H}_2\text{O}$$

$$\Delta P_{\text{matrix}} = 10.2 \text{ in. H}_2\text{O}$$

$$P_a = 30.21 \text{ in. Hg}_a \text{ (atmospheric pressure)}$$

$$d = 2.310 \text{ in. (orifice diameter)}$$

$$D = 3.08 \text{ in. (pipe diameter)}$$

$$t_1 - t_{f1} = 2.73 \text{ mv (initial temperature difference, 5 thermocouples)}$$

$$\text{chart speed} = 2.0 \text{ sec/in}$$

$$\text{chart scale} = 0.558 \text{ mv/in}$$

$$\text{max. slope} = -6.772 \text{ in/in}$$

$$W_s = 0.334 \text{ lbm (matrix mass) (Table VIII)}$$

$$c_s = 0.216 \text{ BTU/lbm }^{\circ}\text{F. (matrix specific heat) (Table VIII)}$$

$$D_h = 0.0035 \text{ ft. (matrix hydraulic diameter) (Table VIII)}$$

$$A_c = 0.0594 \text{ ft}^2 \text{ (matrix flow area) (Table VIII)}$$

$$a = 43.40 \text{ ft}^2 \text{ (matrix heat transfer area) (Table VIII)}$$

Flow Rate Determination

Using the method in (3), the fluid flow rate will be found

$$w_f = 359 K d^2 F_a Y \sqrt{\rho \Delta P_{\text{orifice}}}, \text{ lbm/hr} \quad \left[(3), \text{ p. 57, equation 3} \right]$$

K = flow coefficient, velocity of approach factor included
(dimensionless)

F_a = thermal expansion factor (dimensionless)

Y = expansion factor (dimensionless)

ρ = density of fluid flowing at inlet side of orifice (lbm/ft^3)

R_D = Reynolds number based on pipe diameter

$$\beta = d/D = 0.75$$

assuming $R_D = 94,000$

$$K = 0.7473, \quad [(3), \text{ p. 26, Table 5}]$$

$$d^2 = 5.336 \text{ in}^2$$

$$Y = 0.9959 \quad [(3), \text{ p. 71, Fig. 40B}]$$

$$\rho = 0.756 \text{ lbm}/\text{ft}^3 \quad \frac{P_2}{RT_1} = \frac{(30.21)(491)(144)}{(53.3)(530)} = .0756 \text{ lbm}/\text{ft}^3$$

$$F_a = 1.000 \quad [(3), \text{ p. 67, Fig. 38}]$$

$$w_f = (359)(0.7473)(5.336)(1.000)(0.9959) \sqrt{(0.0756)(4.62)} \\ = 839 \text{ lbm}/\text{hr}$$

$$R_D = 0.004244 w_f/D\mu \quad [(3) \text{ p. 58, equation 8}]$$

$$\mu = 1.225 \times 10^{-5} \text{ lbm}/\text{ft}\cdot\text{sec, at } 70^\circ\text{F,} \quad [(10), \text{ p. 69} \\ \text{Table 2-8}]$$

$$R_D = (0.004244)(839)/(3.08)(1.225 \times 10^{-5}) = 94,326$$

The value of $R_D = 94,326$ does not change the initial flow coefficient.

NTU Determination

To obtain NTU, it is necessary to determine the experimental maximum slope of the generalized slope of the generalized heating curve:

$$\left[\frac{d\left(\frac{t_{f2} - t_i}{t_{f1} - t_i}\right)}{d(T/NTU)} \right]_{\text{MAX}}$$

From the definitions

$$\tau = \frac{hA}{W_s c_s} \left(\theta - \frac{W_f}{w_f} \right)$$

and

$$NTU = \frac{hA}{w_f c_f}$$

then

$$\tau/NTU = \frac{w_f c_f}{W_s c_s} \left(\theta - \frac{W_f}{w_f} \right)$$

and

$$d(\tau/NTU) = \left(\frac{w_f c_f}{W_s c_s} \right) d\theta.$$

Also

$$\frac{t_{f2} - t_i}{t_{f1} - t_i} = \frac{t_{f2} - t_{f1}}{t_{f1} - t_i} + 1$$

and

$$d\left(\frac{t_{f2} - t_i}{t_{f1} - t_i}\right) = \frac{1}{(t_{f1} - t_i)} d(t_{f2} - t_{f1}).$$

Thus the expression for the maximum slope becomes

$$\left[\frac{d\left(\frac{t_{f2} - t_i}{t_{f1} - t_i}\right)}{d(\tau/NTU)} \right]_{\text{MAX}} = \left(\frac{W_s c_s}{w_f c_f} \right) \frac{1}{t_{f1} - t_i} \left[\frac{d(t_{f2} - t_{f1})}{d\theta} \right]_{\text{MAX}}$$

where the quantity

$$\left[\frac{d(t_{f2} - t_{f1})}{d\theta} \right]_{\text{MAX}}$$

is the maximum slope of the inlet-outlet fluid temperature difference versus time curve. As this temperature difference is recorded as a function of time, the maximum slope is determined directly from the experimental trace. Since the slope is measured directly from the chart, in the computations it is necessary to introduce the chart scale-factors.

$$c_f = 0.2404 \text{ BTU/lbm } ^\circ\text{F, fluid specific heat at } 70 ^\circ\text{F,} \\ \text{[(10), p. 41, Table 2-3]}$$

$$\frac{W_s c_s}{\omega_f c_f} = \frac{(0.334)(0.216)(3600)}{(839)(0.2404)} \\ = 1.289 \text{ sec}$$

$$\left[\frac{d\left(\frac{t_{f2} - t_i}{t_{f1} - t_i}\right)}{d\left(\frac{NTU}{NTU}\right)} \right]_{\text{MAX}} = \frac{(1.289)}{-(2.73)} (-6.772) \left[\frac{0.558}{2} \right]_{\text{SF}} = 0.8924$$

$$NTU = 9.165 \text{ (Table IX - Appendix II)}$$

Average fluid temperature determination

$$t_{f1} = 70 ^\circ\text{F.} = 1.07 \text{ mv}$$

$$t_i - t_{f1} = 2.73 \text{ mv (5 thermocouples)}$$

$$t_i - t_{f1} = \frac{t_i - t_{f1}}{5} = \frac{2.73}{5} = 0.546 \text{ mv (1 thermocouple)}$$

$$t_i = (t_i - t_{f1}) + t_{f1} = 0.546 + 1.07 = 1.616 \text{ mv} = 88.87 ^\circ\text{F}$$

$$t_{\text{avg.}} = \frac{t_i + t_{f1}}{2} = \frac{70 + 88.87}{2} = 97.44 ^\circ\text{F}$$

Heat transfer Parameter Determination

$$N_{St} = NTU \frac{Ac}{A} = \frac{(9.165)(0.0594)}{43.40} = 0.0126$$

$$N_{Pr}^{2/3} = 0.795, \text{ at } t_{\text{avg.}} \quad \text{[(10), p. 41, Table 2-10]}$$

$$N_{St} N_{Pr}^{2/3} = (0.0126)(0.795) = 0.00998$$

Reynolds Number Determination

$$N_{Re} = \frac{D_p \bar{v}}{\mu_f}$$

$$\bar{v} = \frac{w_f}{A_c} = (339)(3600)/(0.0594) = 3.92 \text{ lbm/sec-ft}^2$$

$$\mu_f = 1.225 \times 10^{-5} \text{ lbm/ft-sec, at } t_{avg} \quad [(10), \text{ p. 62, Table 2-8}]$$

$$N_{Re} = (0.00135)(3.92) / (1.225 \times 10^{-5}) = 432$$

Friction Factor Determination

$$f = \left(\frac{\Delta P_{matrix}}{v_f} \right) \left(\frac{2g_c}{G^2} \right) \left(\frac{A_c}{L} \right)$$

The friction data were taken at ambient air temperatures.

$$\rho_f = \frac{1}{v_f} = \frac{P_{avg}}{R T_{fi}}$$

$$P_{avg} = P_1 - \frac{\Delta P_{matrix}}{2}$$

$$P_{avg} = (30.2)(13.6) - 10.2/2 = 405.9 \text{ in. H}_2\text{O}$$

$$\rho_f = (405.9)(5.204)/(53.3)(530) = .0747 \text{ lbm/ft}^3$$

$$f = (10.2)(5.204)(0.0747)(2)(32.2)(0.0594) / (3.92)^2(13.6) \\ = 0.0225$$

APPENDIX II

SOLUTION FOR THE MAXIMUM SLOPE OF THE GENERALIZED HEATING CURVE

Locke (1) derived the expression for the slope of the generalized heating curve equation (page 7), noting that when $x = L$ that $Z = NTU$,

$$\frac{d\left(\frac{T_2 - T_1}{T_1 - T_2}\right)}{d(T/NTU)} = \frac{NTU}{\sqrt{NTU^2 + T}} \left[I_1(2\sqrt{NTUT}) e^{-(NTU + T)} \right]$$

A CDC 1604 digital computer was used to solve the equation.

Values of $\left[\frac{d\left(\frac{T_2 - T_1}{T_1 - T_2}\right)}{d(T/NTU)} \right]$ were obtained by

varying T/NTU for particular values of NTU . For values of $NTU \leq 2$, and using an increment of $T/NTU = .00001$, the maximum slope was obtained at the initial value of T/NTU effectively giving

$$\left[\frac{d\left(\frac{T_2 - T_1}{T_1 - T_2}\right)}{d(T/NTU)} \right]_{MAX} = \left(\frac{NTU}{2T} \right)$$

For $NTU > 2$, increments of $T/NTU = .001$ were used. T/NTU was increased until a value of the slope smaller than the previous value was obtained, and this maximum slope was recorded. The computer then moved to the next value of NTU .

The values of $\left[\frac{d\left(\frac{T_2 - T_1}{T_1 - T_2}\right)}{d(T/NTU)} \right]_{MAX}$ for values of NTU and T/NTU are contained in Table II.

Table IX

Values of the Max. Slope of the Generalized Heating Curve, NTU and %NTU

$\left[\frac{(t_h - t_c)}{d(\%NTU)} \right]_{max}$	NTU	$\%NTU$	$\left[\frac{(t_h - t_c)}{d(\%NTU)} \right]_{max}$	NTU	$\%NTU$	$\left[\frac{(t_h - t_c)}{d(\%NTU)} \right]_{max}$	NTU	$\%NTU$	$\left[\frac{(t_h - t_c)}{d(\%NTU)} \right]_{max}$	NTU	$\%NTU$
0.00099	-0.01	0.0001	4.94182	1.45	0.0001	5.71957	2.91	0.0201	6.53042	4.37	0.2800
0.00099	-0.02	0.0001	4.95035	1.46	0.0001	5.72466	2.92	0.0400	6.56004	4.38	0.2900
0.00099	-0.05	0.0001	4.96844	1.47	0.0001	5.72977	2.93	0.0700	6.54166	4.39	0.3000
0.00157	-0.04	0.0001	4.97616	1.48	0.0001	5.73494	2.94	0.0900	6.54729	4.40	0.3100
0.002374	-0.05	0.0001	5.00349	1.49	0.0001	5.74003	2.95	0.1200	6.55290	4.41	0.3200
0.003590	-0.06	0.0001	5.02641	1.50	0.0001	5.74519	2.96	0.1400	6.55851	4.42	0.3300
0.00507	-0.07	0.0001	5.05695	1.51	0.0001	5.75035	2.97	0.1700	6.56412	4.43	0.3400
0.00704	-0.08	0.0001	5.055310	1.52	0.0001	5.75554	2.98	0.1900	6.56974	4.44	0.3500
0.017403	-0.09	0.0001	5.06987	1.53	0.0001	5.76073	2.99	0.2100	6.57534	4.45	0.3600
0.00404	-0.10	0.0001	5.08424	1.54	0.0001	5.76594	3.00	0.2400	6.58095	4.46	0.3700
0.011440	-0.12	0.0001	5.09924	1.55	0.0001	5.77117	3.01	0.2600	6.58656	4.47	0.3800
0.01277	-0.14	0.0001	5.11385	1.56	0.0001	5.77641	3.02	0.2900	6.59216	4.48	0.3900
0.014440	-0.15	0.0001	5.12809	1.57	0.0001	5.78166	3.03	0.3100	6.59776	4.49	0.4000
0.01703	-0.16	0.0001	5.14195	1.58	0.0001	5.78693	3.04	0.3300	6.60336	4.50	0.4100
0.01966	-0.18	0.0001	5.15543	1.59	0.0001	5.79220	3.05	0.3500	6.60896	4.51	0.4200
0.02115	-0.19	0.0001	5.16853	1.60	0.0001	5.79749	3.06	0.3700	6.61455	4.52	0.4300
0.02452	-0.17	0.0001	5.18127	1.61	0.0001	5.80277	3.07	0.4000	6.62014	4.53	0.4400
0.02706	-0.16	0.0001	5.19344	1.62	0.0001	5.80811	3.08	0.4200	6.62573	4.54	0.4500
0.02953	-0.17	0.0001	5.20564	1.63	0.0001	5.81343	3.09	0.4400	6.63132	4.55	0.4600
0.03204	-0.18	0.0001	5.21727	1.64	0.0001	5.81874	3.10	0.4600	6.63691	4.56	0.4700
0.03457	-0.19	0.0001	5.22854	1.65	0.0001	5.82411	3.11	0.4800	6.64249	4.57	0.4800
0.03710	-0.20	0.0001	5.23954	1.66	0.0001	5.82947	3.12	0.5000	6.64807	4.58	0.4900
0.042031	-0.23	0.0001	5.25001	1.67	0.0001	5.83484	3.13	0.5300	6.65365	4.59	0.5000
0.045310	-0.24	0.0001	5.26020	1.68	0.0001	5.84021	3.14	0.5500	6.65923	4.60	0.5100
0.04867	-0.25	0.0001	5.27025	1.69	0.0001	5.84559	3.15	0.5700	6.66480	4.61	0.5200
0.052123	-0.26	0.0001	5.27954	1.70	0.0001	5.85094	3.16	0.5900	6.67038	4.62	0.5300
0.055650	-0.27	0.0001	5.28864	1.71	0.0001	5.85624	3.17	0.6100	6.67595	4.63	0.5400
0.059253	-0.28	0.0001	5.29754	1.72	0.0001	5.86154	3.18	0.6300	6.68151	4.64	0.5500
0.062929	-0.29	0.0001	5.30624	1.73	0.0001	5.86684	3.19	0.6500	6.68707	4.65	0.5600
0.066674	-0.30	0.0001	5.31474	1.74	0.0001	5.87214	3.20	0.6700	6.69263	4.66	0.5700
0.070484	-0.31	0.0001	5.32304	1.75	0.0001	5.87744	3.21	0.6900	6.69819	4.67	0.5800
0.074357	-0.32	0.0001	5.33114	1.76	0.0001	5.88274	3.22	0.7100	6.70374	4.68	0.5900
0.078294	-0.33	0.0001	5.33904	1.77	0.0001	5.88804	3.23	0.7300	6.70929	4.69	0.6000
0.082280	-0.34	0.0001	5.34674	1.78	0.0001	5.89334	3.24	0.7500	6.71484	4.70	0.6100
0.086324	-0.35	0.0001	5.35424	1.79	0.0001	5.89864	3.25	0.7700	6.72038	4.71	0.6200
0.090430	-0.36	0.0001	5.36154	1.80	0.0001	5.90394	3.26	0.7900	6.72592	4.72	0.6300
0.094601	-0.37	0.0001	5.36864	1.81	0.0001	5.90924	3.27	0.8100	6.73146	4.73	0.6400
0.098837	-0.38	0.0001	5.37554	1.82	0.0001	5.91454	3.28	0.8300	6.73699	4.74	0.6500
0.103139	-0.39	0.0001	5.38224	1.83	0.0001	5.91984	3.29	0.8500	6.74252	4.75	0.6600
0.107507	-0.40	0.0001	5.38874	1.84	0.0001	5.92514	3.30	0.8700	6.74804	4.76	0.6700
0.111941	-0.41	0.0001	5.39504	1.85	0.0001	5.93044	3.31	0.8900	6.75356	4.77	0.6800
0.116441	-0.42	0.0001	5.39954	1.86	0.0001	5.93574	3.32	0.9100	6.75907	4.78	0.6900
0.121007	-0.43	0.0001	5.40324	1.87	0.0001	5.94104	3.33	0.9300	6.76457	4.79	0.7000
0.125739	-0.44	0.0001	5.40624	1.88	0.0001	5.94634	3.34	0.9500	6.77006	4.80	0.7100
0.130537	-0.45	0.0001	5.40854	1.89	0.0001	5.95164	3.35	0.9700	6.77554	4.81	0.7200
0.135401	-0.46	0.0001	5.41014	1.90	0.0001	5.95694	3.36	0.9900	6.78101	4.82	0.7300
0.140331	-0.47	0.0001	5.41104	1.91	0.0001	5.96224	3.37	1.0100	6.78647	4.83	0.7400
0.145327	-0.48	0.0001	5.41124	1.92	0.0001	5.96754	3.38	1.0300	6.79192	4.84	0.7500
0.150389	-0.49	0.0001	5.41074	1.93	0.0001	5.97284	3.39	1.0500	6.79736	4.85	0.7600
0.155517	-0.50	0.0001	5.40944	1.94	0.0001	5.97814	3.40	1.0700	6.80279	4.86	0.7700
0.160711	-0.51	0.0001	5.40724	1.95	0.0001	5.98344	3.41	1.0900	6.80820	4.87	0.7800
0.165971	-0.52	0.0001	5.40414	1.96	0.0001	5.98874	3.42	1.1100	6.81360	4.88	0.7900
0.171297	-0.53	0.0001	5.40014	1.97	0.0001	5.99404	3.43	1.1300	6.81899	4.89	0.8000
0.176689	-0.54	0.0001	5.39524	1.98	0.0001	5.99934	3.44	1.1500	6.82437	4.90	0.8100
0.182147	-0.55	0.0001	5.38944	1.99	0.0001	6.00464	3.45	1.1700	6.82974	4.91	0.8200
0.187671	-0.56	0.0001	5.38274	2.00	0.0001	6.01004	3.46	1.1900	6.83509	4.92	0.8300
0.193261	-0.57	0.0001	5.37514	2.01	0.0001	6.01544	3.47	1.2100	6.84043	4.93	0.8400
0.198917	-0.58	0.0001	5.36664	2.02	0.0001	6.02084	3.48	1.2300	6.84576	4.94	0.8500
0.204639	-0.59	0.0001	5.35724	2.03	0.0001	6.02624	3.49	1.2500	6.85108	4.95	0.8600
0.210427	-0.60	0.0001	5.34694	2.04	0.0001	6.03164	3.50	1.2700	6.85639	4.96	0.8700
0.216281	-0.61	0.0001	5.33574	2.05	0.0001	6.03704	3.51	1.2900	6.86169	4.97	0.8800
0.222201	-0.62	0.0001	5.32364	2.06	0.0001	6.04244	3.52	1.3100	6.86698	4.98	0.8900
0.228187	-0.63	0.0001	5.31064	2.07	0.0001	6.04784	3.53	1.3300	6.87226	4.99	0.9000
0.234239	-0.64	0.0001	5.29674	2.08	0.0001	6.05324	3.54	1.3500	6.87753	5.00	0.9100
0.240357	-0.65	0.0001	5.28194	2.09	0.0001	6.05864	3.55	1.3700	6.88279	5.01	0.9200
0.246541	-0.66	0.0001	5.26624	2.10	0.0001	6.06404	3.56	1.3900	6.88804	5.02	0.9300
0.252791	-0.67	0.0001	5.24964	2.11	0.0001	6.06944	3.57	1.4100	6.89328	5.03	0.9400
0.259107	-0.68	0.0001	5.23214	2.12	0.0001	6.07484	3.58	1.4300	6.89851	5.04	0.9500
0.265489	-0.69	0.0001	5.21374	2.13	0.0001	6.08024	3.59	1.4500	6.90373	5.05	0.9600
0.271937	-0.70	0.0001	5.19444	2.14	0.0001	6.08564	3.60	1.4700	6.90894	5.06	0.9700
0.278451	-0.71	0.0001	5.17424	2.15	0.0001	6.09104	3.61	1.4900	6.91414	5.07	0.9800
0.285031	-0.72	0.0001	5.15314	2.16	0.0001	6.09644	3.62	1.5100	6.91933	5.08	0.9900
0.291677	-0.73	0.0001	5.13114	2.17	0.0001	6.10184	3.63	1.5300	6.92451	5.09	1.0000
0.298389	-0.74	0.0001	5.10824	2.18	0.0001	6.10724	3.64	1.5500	6.92968	5.10	1.0100
0.305167	-0.75	0.0001	5.08444	2.19	0.0001	6.11264	3.65	1.5700	6.93484	5.11	1.0200
0.312011	-0.76	0.0001	5.05974	2.20	0.0001	6.11804	3.66	1.5900	6.94000	5.12	1.0300
0.318921	-0.77	0.0001	5.03414	2.21	0.0001	6.12344	3.67	1.6100	6.94515	5.13	1.0400
0.325897	-0.78	0.0001	5.00764	2.22	0.0001	6.12884	3.68	1.6300	6.95029	5.14	1.0500
0.332939	-0.79	0.0001	4.98024	2.23	0.0001	6.13424	3.69	1.6500	6.95543	5.15	1.0600
0.340047	-0.80	0.0001	4.95194	2.24	0.0001	6.13964	3.70	1.6700	6.96056	5.16	1.0700
0.347221	-0.81	0.0001	4.92274	2.25	0.0001	6.14504	3.71	1.6900	6.96568	5.17	1.0800
0.354461	-0.82	0.0001	4.89264	2.26	0.0001	6.15044	3.72	1.7100	6.97079	5.18	1.0900
0.361767	-0.83	0.0001	4.86174	2.27	0.0001	6.15584	3.73	1.7300	6.97589	5.19	1.1000
0.369139	-0.84	0.0001	4.83004	2.28	0.0001	6.16124	3.74	1.7500	6.98098	5.20	1.1100
0.376577	-0.85	0.0001	4.79754	2.29	0.0001	6.16664	3.75	1.7700	6.98606	5.21	1.1200
0.384081	-0.86	0.0001	4.76424	2.30	0.0001	6.17204	3.76	1.7900	6.99113	5.22	1.1300
0.391651	-0.87	0.0001	4.73014	2.31	0.0001	6.17744	3.77	1.8100	6.99619	5.23	1.1400
0.399287	-0.88	0.0001	4.69524	2.32	0.0001	6.18284	3.78	1.8300	7.00124	5.24	1.1500
0.406989	-0.89	0.0001	4.65954	2.33	0.0001	6.18824	3.79	1.8500	7.00628	5.25	1.1600
0.414757	-0.90	0.0001	4.62304	2.34	0.0001	6.19364	3.80	1.8700	7.01131	5.26	1.170

DUDLEY KNOX LIBRARY - RESEARCH REPORTS



5 6853 01076956 5

thesM386

DUDLEY KNOX LIBRARY



3 2768 00416491 3

DUDLEY KNOX LIBRARY